Nanolock-nanopore facilitated digital diagnostics of cancer driver mutation in tumor tissue

Yong Wang[1,2†], Kai Tian[1,2†], Ruicheng Shi[1,2], Amy Gu[2], Michael Pennella[2], Lindsey Alberts[1], Kent S. Gates[3,4], Guangfu Li[5,6], Hongxin Fan[7], Michael X. Wang[8,9], Li-Qun Gu[1,2]*

[1]Department of Bioengineering and [2]Dalton Cardiovascular Research Center, University of Missouri, Columbia, MO 65211, USA

[3]Department of Chemistry and [4]Department of Biochemistry, 125 Chemistry Building, University of Missouri, Columbia, MO 65211, USA

[5]Department of Surgery and [6]Ellis Fischel Cancer Center, University of Missouri, Columbia, MO 65212, USA.

[7]Department of Pathology, University of Texas Health Science Center at San Antonio, San Antonio, TX 78229, USA

[8]Department of Pathology and Anatomical Sciences and [9]Department of Computer Science, University of Missouri, Columbia, MO 65211, USA

Supplementary Information

Table S1 – S2

Figure S1 – S5

Supplementary Information S1 – S4

Table S1. Sequences of DNAs used in this study

DNA	Sequence (5'→3')
Forward primer	TCATAATGCTTGCTCTGATAGGA
Reverse primer	GGCCAAAAATTTAATCAGTGGA
224-bp amplicon [a] (sense strand)	TCATAATGCTTGCTCTGATAGGAAAATGAGATCTACTGTTTTCCTT TACTTACTACACCTCAG(ATATATTTCTTCATGAAGACCTCACAGT AAAAATAGGTGATTTTGGTCTAGCTACAG**N**GAAATCTCGATGGAGT GGGTCCCATCAGTTTGAACAGTTGTCTGGATCCATTTTGTGGATGG)TAAGAATTGAGGCTATTTTTCCACTGATTAAATTTTTGGCC
(antisense strand)	GGCCAAAAATTTAATCAGTGGAAAAATAGCCTCAATTCTTA(CCAT CCACAAAATGGATCCAGACAACTGTTCAAACTGATGGGACCCACTC CATCGAGATTTC**N**CTGTAGCTAGACCAAAATCACCTATTTTTACTG TGAGGTCTTCATGAAGAAATATAT)CTGAGGTGTAGTAAGTAAAGG AAAACAGTAGATCTCATTTTCCTATCAGAGCAAGCATTATGA
T^{wt} (target, antisense)	CGAGATTTC**A**CTGTAGC
T^{V600E} (target, antisense)	CGAGATTTC**T**CTGTAGC
P (probe)	GCTACAG**T**GAAATCTCG
P' (probe) [b]	GCTACAG**A**GAAATCTCG

[a]: The fragment enclosed in the brackets is Exon 15 of the *BRAF* gene. Bolded code N at the position 1799 is the V600E mutation site, which is a T in the sense strand and A in the antisense strand for the wild-type allele, and A in the sense strand and T in the antisense strand for the V600E mutant allele. The underlined and double-underlined codes are the cleavage sites for *Bfa*I and *Taq*I, respectively. The digestion products are the targets T^{wt} and T^{V600E}.

[b]: P' is the fully complementary strand of T^{V600E}, cannot form the nanolock.

Table S2. Case information of thyroid cancer patients [a]

Sample#	Diagnosis	Tumor cell % on slide
13-043	Papillary Carcinoma	10
13-117	Papillary Carcinoma	30
13-119	Papillary Carcinoma	90

[a]: DNA extraction from tumor tissues is described in Methods

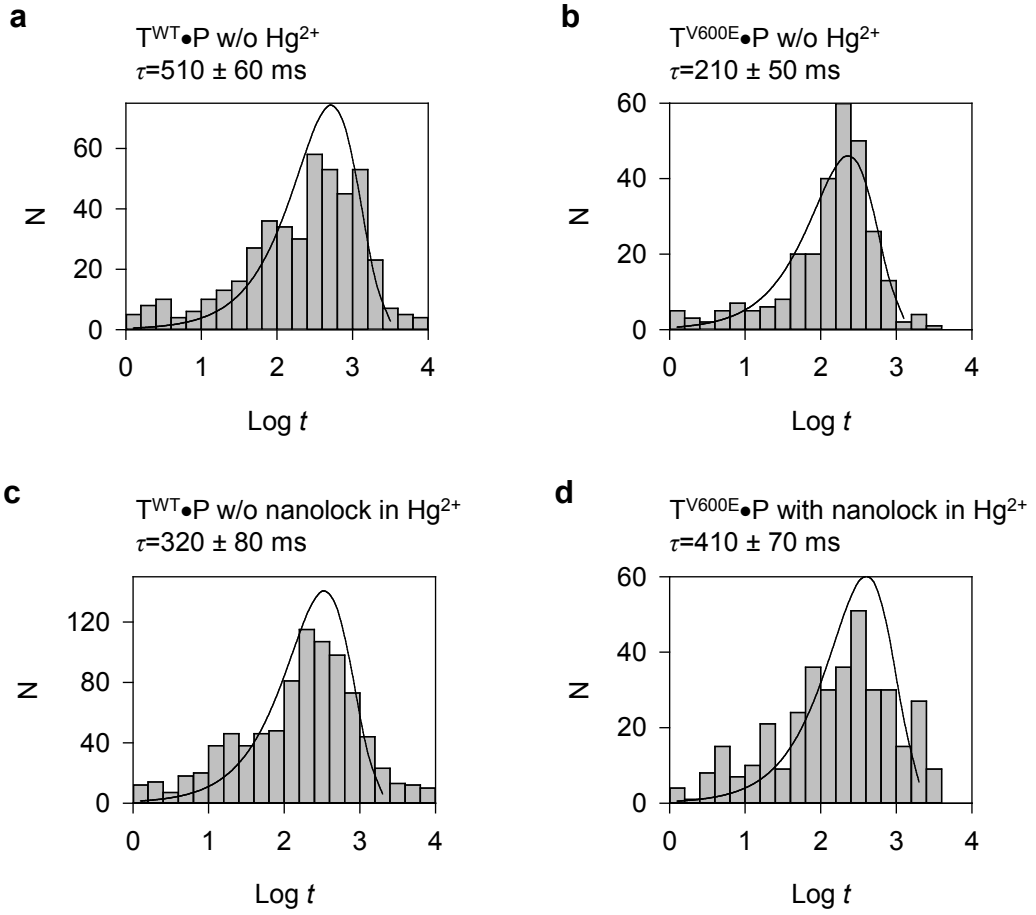

Figure S1. Histograms of block duration recorded for various DNA duplexes without and with interaction with Hg^{2+}. **a-d,** Histograms produced by T^{WT}•P (a) and T^{V600E}•P (b) duplex in the absence of Hg^{2+}, and T^{WT}•P (c) and T^{V600E}•P (d) duplex in the absence of Hg^{2+}. Note that the x-axis log *t* is the duration in the log scale. The unit labels, 0, 1, 2, 3 and 4, represent 1, 10, 100, 1,000, and 10,000 ms; y-axis *N* is the count number of single-molecule events. The exponential distribution of block duration was fitted using $N=P\cdot\exp(\ln t-\ln\tau-\exp(\ln t-\ln\tau))$. The block duration was obtained from current traces recorded at +180 mV in 1 M KCl and 10 mM Tris (pH7.2).

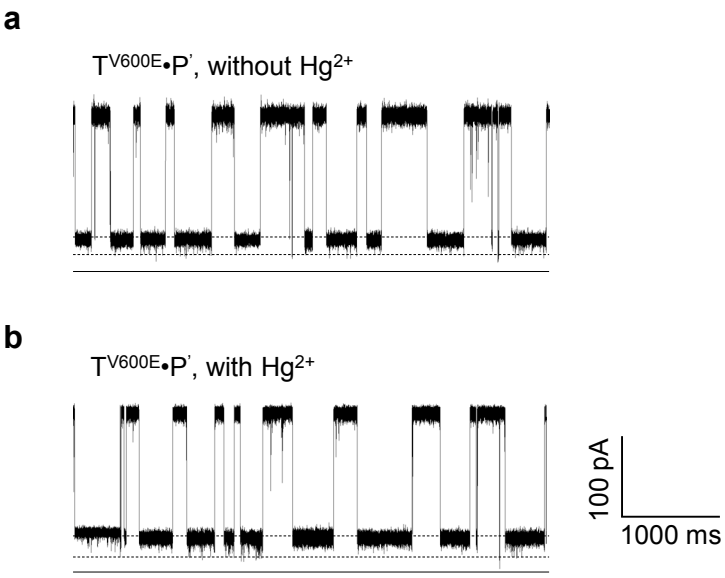

Figure S2. Nanopore current blocks by the T^{V600E}•P'duplex in the absence (top) and in the presence of Hg^{2+} (bottom). As P' (Table S1) does not form T-T base pair with T^{V600E}, the T^{V600E}•P'duplex does not form the T-Hg-T nanolock. Experimentally, the characteristic stepwise e-marker blocks were not observed in the presence of Hg^{2+}, supporting that the T^{V600E}•P' duplex does not form the nanolock.

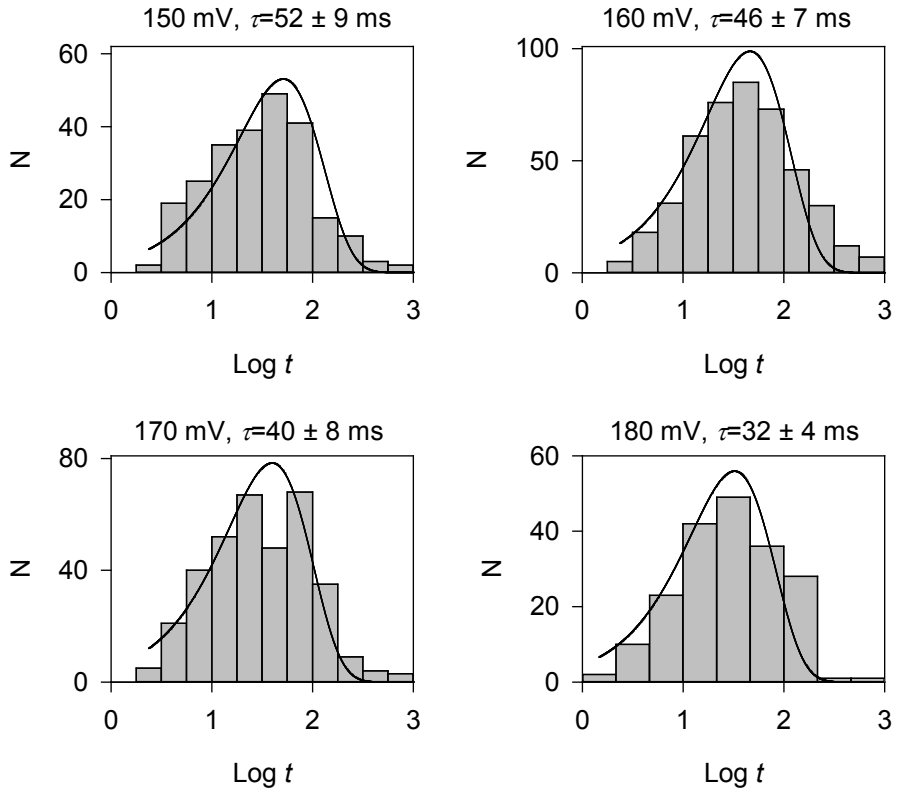

Figure S3. Histograms of the Level B duration in the stepwise block produced by the T^{V600E}•P duplex with a nanolock (Fig. 2f) at various voltages. The x-axis log *t* is the duration in the log scale, so the unit labels, 0, 1, 2, 3 and 4, represent 1, 10, 100, 1,000, and 10,000 ms; y-axis *N* is the count number of single-molecule events. The distribution was fitted using a function as described in Fig. S1.

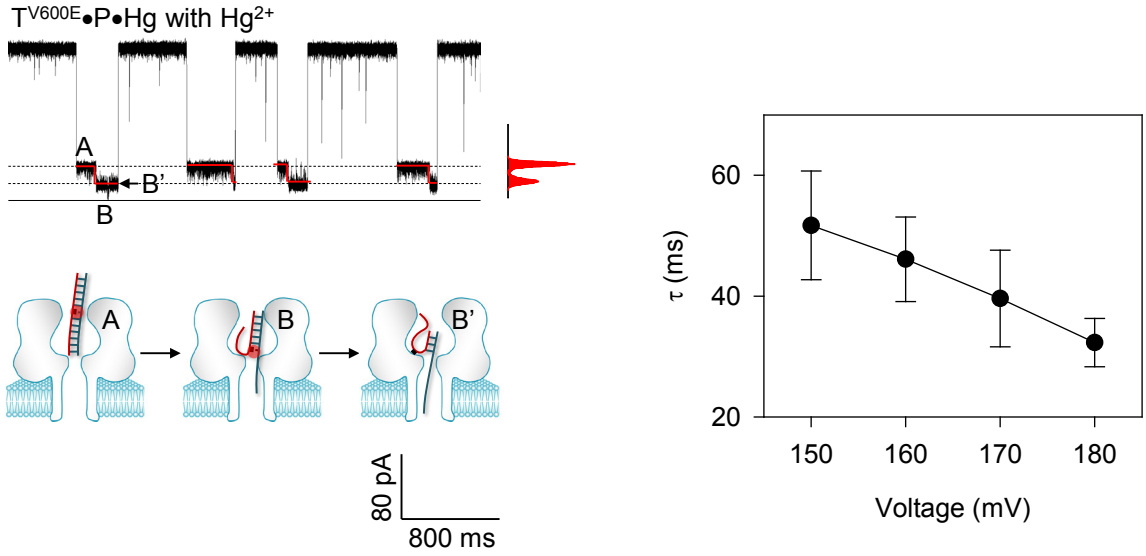

Figure S4. Voltage dependence of the Level B duration for the T^{V600E}•P duplex carrying a nanolock. Histograms of durations were analyzed in Fig. S2. The Level B duration was shortened as the voltage increased, supporting the dissociation of the nanolock in the T^{V600E}•P duplex.

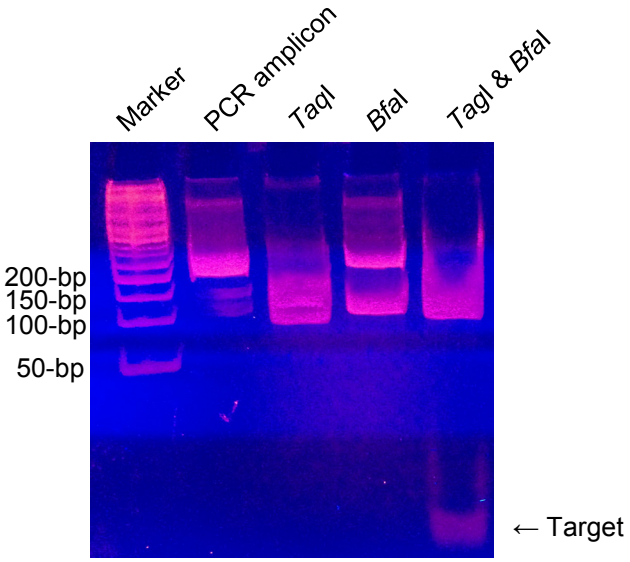

Figure S5. Electrophoretic illustration of PCR/digestion products of tumor DNAs. Tumor DNA was extracted from a Papillary Carcinoma tissue sample with 50% tumor percentage. The gel image shows the bands for the 224-bp amplicon after PCR, the digestion fragments after treatment of the amplicon with *Bfa*I, *Taq*I, and both enzymes. The target fragment after digestion with both enzymes is identified in the gel. The electrophoresis was run on a 12% polyacrylamide gel. The electrophoresis is to reveal the PCR and digestion efficiency, but is not included in the mutation detection protocol.

S1. Oncogenic driver mutation, *BRAF* V600E mutation, and current detection methods. Oncogenic gene alterations, or driver mutations, are hallmarks of genetic determinants in cancer. Most of these genetic changes are single-nucleotide substitution (point mutations)[1], and contribute to tumor initiation and progression through conferring growth advantage on the cancer cells[2]. As such, driver mutations are cancer diagnostic biomarkers and therapeutic targets. The serine/threonine-protein kinase *BRAF* has a series of oncogenic variants. *BRAF* V600E (1799T>A) is a clinically significant driver mutation that has been detected with high prevalence in many types of cancers[3], including 50% of melanomas[4-10], 45% of papillary thyroid carcinomas[11-14], and 100% of hairy cell leukemias[15], as well as many other cancers[16-18] such as colorectal carcinoma[15] and pleomorphic xanthoastrocytoma[19, 20]. The mutated BRAF protein is "locked" in an activated state, resulting in persistent oncogenic signaling through the MEK/ERK pathway[21]. This oncogenic mechanism makes *BRAF* an attractive therapeutic target. Various tyrosine kinase inhibitors, such as vemurafenib and dabrafenib, have been successfully used to target *BRAF* V600E positive cancers with remarkable efficacy. Therefore, *BRAF* V600E is a biomarker with significant diagnostic, therapeutic and prognostic implications. Accurate detection and quantification of driver mutations is important to precision oncology, allowing cancer patients to receive individually tailored treatments[22].

A popular method for point mutation detection is real-time PCR (RT-PCR). A few companion tests have been approved by FDA for clinical use to detect *BRAF* V600E mutation in DNA samples extracted from formalin-fixed paraffin-embedded (FFPE) human melanoma tissue[23-25]. These approved tests are qualitative assays, and are intrinsically prone to contamination to generate a false-positive result even for a mutation-free sample, or a poor PCR reaction due to DNA fragmentation from FFPE tissue produces a false-negative result[26, 27].

Moreover, the expensive instrumentation and reagents increase the cost in clinical laboratories. Emerging new methods for *BRAF* mutant detection include quantum dots[28], ligase and luminescence resonance energy transfer[29], silicon[30] and gold nanowires[31], atomic force cantilever arrays[32], and cycling temperature capillary electrophoresis[33]. Most of these methods, which have been tested for synthetic nucleic acids and cell lines, have yet to be validated in clinical samples.

S2. Quantification of the *BRAF* V600E mutation percentage in tumor DNAs. The e-marker and non-marker blocks for DNA unzipping are at the time scale of 10-100 ms. Meanwhile the short block for rapid translocation of single-stranded DNA was at the 100 μs level, and were excluded from the counting of e-markers and non-marker blocks by using 1 ms cut-off duration.

The e-marker for the T^{V600E}•P duplex carrying a nanopore undergoes stepwise unzipping in the nanopore. The frequency of e-marker can be determined by

$$f_+ = k_{on} A P_1 [T^{V600E}] \qquad (S1)$$

where $[T^{V600E}]$ is the concentration of the V600E target fragment; P_1 is the fraction of T^{V600E} that is hybridized with the probe, thus $P_1[T^{V600E}]$ is the concentration of the T^{V600E}•P hybrid; A is yield of the interstrand lock, i.e. the fraction of the B^{V600E}•P hybrid that forms a nanolock with Hg^{2+}, thus $AP_1[T^{V600E}]$ gives the concentration of the T^{V600E}•P•Hg complex; k_{on} is the capture rate of the DNA duplex in the nanopore, thus $k_{on}AP_1[B^{V600E}]$ is the frequency of signature blocks generated by the B^{V600E}•P•Hg complex.

The non-marker blocks are contributed by the T^{WT}•P duplex and free T^{V600E}•P hybrid without nanlock. Its frequency can be expressed as

$$f_- = k_{on}(1 - A_1)P_1[T^{V600E}] + k_{on}P_2[T^{WT}] \qquad (S2)$$

Where $[T^{V600E}]$ and $[T^{WT}]$ are the concentrations of the V600E and wild-type target; P_1 and P_2 are the fractions of T^{V600E} and T^{WT} that are hybridized with the probe, thus $P_1[T^{V600E}]$ and $P_2[T^{WT}]$ represent the concentrations of the T^{V600E}•P and T^{WT}•P duplexes, $(1-A)P_1[T^{V600E}]$ gives the concentration of the free T^{V600E}•P duplex without nanolock, and $k_{on}(1-A)P_1[T^{V600E}]$ gives the frequency of non-marker blocks generated by the T^{V600E}•P complex, and $k_{on}P_2[T^{WT}]$ is the non-marker frequency generated by the T^{WT}•P hybrid.

The number of signature blocks $N+$ and non-signature blocks $N-$ are proportional to the frequency of the two types of blocks,

$$\frac{N_+}{N_-} = \frac{f_+}{f_-} \qquad \text{(S3)}$$

By combining Eq. S1 with S3, we obtain

$$\frac{N_+}{N_-} = \frac{A\left[T^{V600E}\right]}{(1-A)[T^{V600E}] + (P_2/P_1)\left[T^{WT}\right]} \qquad \text{(S4)}$$

When the probe concentration is much higher than the target DNA concentration, most of the target will be hybridized with the probe, thus $P_2/P_1 \approx 1$. If the V600E target percentage $T^{V600E}\%$ is used to replace DNA concentrations $[T^{V600E}]$ and $[T^{WT}]$, we have

$$\frac{N_+}{N_-} = \frac{A \cdot T^{V600E}\%}{(1-A)T^{V600E}\% + (1 - T^{V600E}\%)} \qquad \text{(S5)}$$

The simplified form of Eq. S5 is

$$\frac{N_+}{N_-} = \frac{A \cdot T^{V600E}\%}{1 - A \cdot T^{V600E}\%} \qquad \text{(S6)}$$

As PCR amplifies both wild-type and mutant DNAs with equal opportunity, we assume measured T^{V600E}% can be used to represent the *BRAF* V600E mutation percentage (MT%). Therefore, the correlation of $N+/N-$ and MT% can be expressed as

$$\frac{N_+}{N_-} = \frac{A \cdot \mathrm{MT\%}}{1 - A \cdot \mathrm{MT\%}} \qquad (S7)$$

Eq. S7 was used to determine the $N+/N-$-MT% correlation in Fig. 4b. $N+/N-$ increases from 0 to $A/(1-A)$ as MT% varies from 0% to 100%.

S3. *BRAF* V600E mutation detection by allele-discrimination PCR (AD-PCR). AD-PCR[34, 35] was performed by a validated laboratory developed test on 7900HT fast real-time PCR system (Life Technologies, Carlsbad, CA). The assay is sensitive to detect about 6% of mutant allele and linear from 6% to 100%. Briefly, extracted DNA was amplified with specific forward primer BRAF-51F 5'–CTACTGTTTTCCTTTACTTACTACACCTCAGA–3' and reverse primer BRAF-176R 5'–ATCCAGACAACTGTTCAAACTGATG–3', as well as MGB mutant (MT) probe 5'–FAM–TAGCTACAGaGAAATC–3' and wild-type (WT) probe 5'–VIC–CTAGCTACAGtGAAATC–3'. Primer and probes are cited from literature[34]. The primer set produced a 125 basepairs PCR amplicon.

The PCR reaction contains 900 nM of each primer, 250 nM of each probe, 2× TaqMan Genotyping Master Mix (Life Technologies, Carlsbad, CA), and 40 ng of DNA in a total volume of 20 µl reaction. The PCR program consisted of 45 cycles of denaturation at 95°C for 15 seconds, followed by annealing and elongation at 60°C for 1 minute. Both allele discrimination and real-time amplification data were collected by SDS software version 2.4 (Life Technologies, Carlsbad, CA).

The allelic status (mutant versus wild type) was determined by either WT or MT probe in allelic discrimination plot, and quantity of mutation allele percentage was evaluated by comparing unknown patient sample results to the 100% mutation control – a V600E homozygous melanoma cell line SK-MEL-28 (ATCC# HTB-72D) using the comparative C(t) method[35].

S4. Low detection limit (LDL) of commonly used methods for detection of the *BRAF* V600E mutation. LDL is 5% for the FDA-approved COBAS *BRAF* V600E mutation test (Roche Molecular System Inc, http://molecular.roche.com/assays/Pages/cobas4800BRAFV600MutationTest.aspx), 1% for the B-Raf Codon 600 Mutation Analysis Kit (EntroGen, Inc, http://entrogen.com/web3/b-raf-codon-600-mutation-analysis-kit/), 1-2% for the BRAF RGQ PCR Kit (Qiagen Inc, https://www.qiagen.com/us/shop/assay-technologies/complete-assay-kits/personalized-healthcare/braf-rgq-pcr-kit/), 1-5% for pyro-sequencing, and 20% for Sanger sequencing.

Supplementary references

1. Vogelstein, B.; Papadopoulos, N.; Velculescu, V. E.; Zhou, S.; Diaz, L. A., Jr.; Kinzler, K. W. Cancer genome landscapes. *Science* 2013, 339, 1546-1558.

2. Stratton, M. R.; Campbell, P. J.; Futreal, P. A. The cancer genome. *Nature* 2009, 458, 719-724.

3. Villanueva, M. T. Melanoma: blocking BRAF to the BRIM. *Nature reviews. Clinical oncology* 2014, 11, 179.

4. Dankort, D.; Curley, D. P.; Cartlidge, R. A.; Nelson, B.; Karnezis, A. N.; Damsky, W. E., Jr.; You, M. J.; DePinho, R. A.; McMahon, M.; Bosenberg, M. Braf(V600E) cooperates with Pten loss to induce metastatic melanoma. *Nat Genet* 2009, 41, 544-552.

5. Fedorenko, I. V.; Paraiso, K. H.; Smalley, K. S. Acquired and intrinsic BRAF inhibitor resistance in BRAF V600E mutant melanoma. *Biochem Pharmacol* 2011, 82, 201-209.

6. Hou, P.; Liu, D.; Dong, J.; Xing, M. The BRAF(V600E) causes widespread alterations in gene methylation in the genome of melanoma cells. *Cell Cycle* 2012, 11, 286-295.

7. Kumar, S. M.; Yu, H.; Edwards, R.; Chen, L.; Kazianis, S.; Brafford, P.; Acs, G.; Herlyn, M.; Xu, X. Mutant V600E BRAF increases hypoxia inducible factor-1alpha expression in melanoma. *Cancer Res* 2007, 67, 3177-3184.

8. Park, J. Melanoma-targeted therapy based on V600E BRAF mutation. *Biomark Med* 2010, 4, 792.

9. Yancovitz, M.; Litterman, A.; Yoon, J.; Ng, E.; Shapiro, R. L.; Berman, R. S.; Pavlick, A. C.; Darvishian, F.; Christos, P.; Mazumdar, M.; Osman, I.; Polsky, D. Intra- and inter-tumor heterogeneity of BRAF(V600E))mutations in primary and metastatic melanoma. *PLoS One* 2012, 7, e29336.

10. Gear, H.; Williams, H.; Kemp, E. G.; Roberts, F. BRAF mutations in conjunctival melanoma. *Investigative ophthalmology & visual science* 2004, 45, 2484-2488.

11. Sheu, S. Y.; Grabellus, F.; Schwertheim, S.; Handke, S.; Worm, K.; Schmid, K. W. Lack of correlation between BRAF V600E mutational status and the expression profile of a distinct set

of miRNAs in papillary thyroid carcinoma. *Hormone and metabolic research = Hormon- und Stoffwechselforschung = Hormones et metabolisme* 2009, 41, 482-487.

12. Frasca, F.; Nucera, C.; Pellegriti, G.; Gangemi, P.; Attard, M.; Stella, M.; Loda, M.; Vella, V.; Giordano, C.; Trimarchi, F.; Mazzon, E.; Belfiore, A.; Vigneri, R. BRAF(V600E) mutation and the biology of papillary thyroid cancer. *Endocr Relat Cancer* 2008, 15, 191-205.

13. Rowe, L. R.; Bentz, B. G.; Bentz, J. S. Detection of BRAF V600E activating mutation in papillary thyroid carcinoma using PCR with allele-specific fluorescent probe melting curve analysis. *J Clin Pathol* 2007, 60, 1211-1215.

14. Park, S. Y.; Park, Y. J.; Lee, Y. J.; Lee, H. S.; Choi, S. H.; Choe, G.; Jang, H. C.; Park, S. H.; Park do, J.; Cho, B. Y. Analysis of differential BRAF(V600E) mutational status in multifocal papillary thyroid carcinoma: evidence of independent clonal origin in distinct tumor foci. *Cancer* 2006, 107, 1831-1838.

15. Torigoe, H.; Miyakawa, Y.; Fukushi, M.; Ono, A.; Kozasa, T. Development of a novel device to trap heavy metal cations: application of the specific interaction between heavy metal cation and mismatch DNA base pair. *Nucleic Acids Symp Ser (Oxf)* 2009, 23-24.

16. Li, W. Q.; Kawakami, K.; Ruszkiewicz, A.; Bennett, G.; Moore, J.; Iacopetta, B. BRAF mutations are associated with distinctive clinical, pathological and molecular features of colorectal cancer independently of microsatellite instability status. *Molecular cancer* 2006, 5, 2.

17. Puxeddu, E.; Moretti, S.; Elisei, R.; Romei, C.; Pascucci, R.; Martinelli, M.; Marino, C.; Avenia, N.; Rossi, E. D.; Fadda, G. BRAFV599E mutation is the leading genetic event in adult sporadic papillary thyroid carcinomas. *The Journal of Clinical Endocrinology & Metabolism* 2004, 89, 2414-2420.

18. Tiacci, E.; Trifonov, V.; Schiavoni, G.; Holmes, A.; Kern, W.; Martelli, M. P.; Pucciarini, A.; Bigerna, B.; Pacini, R.; Wells, V. A. BRAF mutations in hairy-cell leukemia. *New England Journal of Medicine* 2011, 364, 2305-2315.

19. Dias-Santagata, D.; Lam, Q.; Vernovsky, K.; Vena, N.; Lennerz, J. K.; Borger, D. R.; Batchelor, T. T.; Ligon, K. L.; Iafrate, A. J.; Ligon, A. H.; Louis, D. N.; Santagata, S. BRAF V600E mutations are common in pleomorphic xanthoastrocytoma: diagnostic and therapeutic implications. *PLoS One* 2011, 6, e17948.

20. Schindler, G.; Capper, D.; Meyer, J.; Janzarik, W.; Omran, H.; Herold-Mende, C.; Schmieder, K.; Wesseling, P.; Mawrin, C.; Hasselblatt, M.; Louis, D. N.; Korshunov, A.; Pfister,

S.; Hartmann, C.; Paulus, W.; Reifenberger, G.; von Deimling, A. Analysis of BRAF V600E mutation in 1,320 nervous system tumors reveals high mutation frequencies in pleomorphic xanthoastrocytoma, ganglioglioma and extra-cerebellar pilocytic astrocytoma. *Acta Neuropathol* 2011, 121, 397-405.

21. Wan, P. T.; Garnett, M. J.; Roe, S. M.; Lee, S.; Niculescu-Duvaz, D.; Good, V. M.; Project, C. G.; Jones, C. M.; Marshall, C. J.; Springer, C. J. Mechanism of activation of the RAF-ERK signaling pathway by oncogenic mutations of B-RAF. *Cell* 2004, 116, 855-867.

22. Bollag, G.; Tsai, J.; Zhang, J.; Zhang, C.; Ibrahim, P.; Nolop, K.; Hirth, P. Vemurafenib: the first drug approved for BRAF-mutant cancer. *Nature Reviews Drug Discovery* 2012, 11, 873-886.

23. Halait, H.; DeMartin, K.; Shah, S.; Soviero, S.; Langland, R.; Cheng, S.; Hillman, G.; Wu, L.; Lawrence, H. J. Analytical performance of a real-time PCR-based assay for V600 mutations in the BRAF gene, used as the companion diagnostic test for the novel BRAF inhibitor vemurafenib in metastatic melanoma. *Diagnostic Molecular Pathology* 2012, 21, 1-8.

24. Jarry, A.; Masson, D.; Cassagnau, E.; Parois, S.; Laboisse, C.; Denis, M. G. Real-time allele-specific amplification for sensitive detection of the BRAF mutation V600E. *Molecular and cellular probes* 2004, 18, 349-352.

25. Sapio, M. R.; Posca, D.; Troncone, G.; Pettinato, G.; Palombini, L.; Rossi, G.; Fenzi, G.; Vitale, M. Detection of BRAF mutation in thyroid papillary carcinomas by mutant allele-specific PCR amplification (MASA). *European Journal of Endocrinology* 2006, 154, 341-348.

26. Tabrizi, S. N.; Unemo, M.; Limnios, A. E.; Hogan, T. R.; Hjelmevoll, S. O.; Garland, S. M.; Tapsall, J. Evaluation of six commercial nucleic acid amplification tests for detection of Neisseria gonorrhoeae and other Neisseria species. *J Clin Microbiol* 2011, 49, 3610-3615.

27. Upton, A.; Bromhead, C.; Whiley, D. M. Neisseria gonorrhoeae false-positive result obtained from a pharyngeal swab by using the Roche cobas 4800 CT/NG assay in New Zealand in 2012. *J Clin Microbiol* 2013, 51, 1609-1610.

28. Ai, X.; Ma, Q.; Su, X. Multiplex DNA sensor for BRAF and BRCA detection. *Analytical biochemistry* 2013, 438, 22-28.

29. Wang, P.; Zhang, P. Ligase-assisted, upconversion luminescence resonance energy transfer-based method for specific and sensitive detection of V600E mutation in the BRAF gene. *RSC Advances* 2014, 4, 56235-56240.

30. Wu, C. C.; Ko, F. H.; Yang, Y. S.; Hsia, D. L.; Lee, B. S.; Su, T. S. Label-free biosensing of a gene mutation using a silicon nanowire field-effect transistor. *Biosensors and Bioelectronics* 2009, 25, 820-825.

31. Fang, Z.; Kelley, S. O. Direct electrocatalytic mRNA detection using PNA-nanowire sensors. *Analytical Chemistry* 2009, 81, 612-617.

32. Huber, F.; Lang, H.; Backmann, N.; Rimoldi, D.; Gerber, C. Direct detection of a BRAF mutation in total RNA from melanoma cells using cantilever arrays. *Nature nanotechnology* 2013, 8, 125-129.

33. Hinselwood, D. C.; Abrahamsen, T. W.; Ekstrøm, P. O. BRAF mutation detection and identification by cycling temperature capillary electrophoresis. *Electrophoresis* 2005, 26, 2553-2561.

34. Benlloch, S.; Paya, A.; Alenda, C.; Bessa, X.; Andreu, M.; Jover, R.; Castells, A.; Llor, X.; Aranda, F. I.; Massuti, B. Detection of BRAF V600E mutation in colorectal cancer: comparison of automatic sequencing and real-time chemistry methodology. *J Mol Diagn* 2006, 8, 540-543.

35. Schmittgen, T. D.; Livak, K. J. Analyzing real-time PCR data by the comparative C(T) method. *Nat Protoc* 2008, 3, 1101-1108.